Journal of Membrane Science 431 (2013) 187–196

Contents lists available at SciVerse ScienceDirect

Journal of Membrane Science

journal homepage: www.elsevier.com/locate/memsci

Deacidification and solvent recovery of soybean oil by nanofiltration membranes

Leticia R. Firman [a], Nelio A. Ochoa [b], José Marchese [b,*], Cecilia L. Pagliero [a]

[a] Facultad de Ingeniería-UNRC – CONICET-FONCYT, Ruta No. 36, Km 601, 5800 Río Cuarto, Argentina
[b] Universidad Nacional de San Luis, INFAP – CONICET-FONCYT, Chacabuco 915, 5700 San Luis, Argentina

ARTICLE INFO

Article history:
Received 22 May 2012
Received in revised form
3 December 2012
Accepted 29 December 2012
Available online 8 January 2013

Keywords:
Nanofiltration
Polymeric membrane
Soybean oil
Solvent recovery
Deacidification

ABSTRACT

Four tailor-made flat composite membranes of poly(vinylideneflouride) (PVDF) as a support and polydimethylsiloxane (PDMS) or cellulose acetate (CA) as coating layer, and a commercially available composite membrane (Solsep 030306) were used to remove hexane and free fatty acid (FFA) from crude soybean oil–hexane mixture. The effects of transmembrane pressure (Δp=10–20 bar), temperature (T=30–50 °C) and feed oil concentration (C_f=10–35 w/w%) on membrane selectivity and permeation flux were determined. The PVDF-12% siloxane composite nanofiltration membrane achieved the best results, being stable in commercial hexane and having promising permselectivity properties to separate soybean oil/hexane miscella. Improved separation performance was obtained at C_f=25%, Δp=20 bar, and T=30 °C, achieving a permeate flux of 20.3 $Lm^{-2}\,h^{-1}$, 80% oil retention, 58% FFA removal.

1. Introduction

Crude edible oils need to be refined to obtain the properties required for their consumption. This procedure involves removing undesirable components and concentrating the desirable ones [1]. Vegetable oils are usually extracted from the oilseeds with hexane. The process includes a step of solvent recovery from miscella (mixture oil/solvent). Extensive and expensive processes, such as double-effect evaporation and steam stripping, are used to remove hexane from oil. The first stage, called an economizer, is designed to remove the majority of the solvent and concentrate the miscella as much as possible (70 to 90% oil). The concentrated miscella is then pumped to the second-stage evaporator (under partial vacuum), where the oil concentration is brought to $>99\%$ ($<1\%$ hexane) [2].

Several studies focus on the development of new oil purification, deacidification, discolouration and solvent recovery methods. Membrane processes have gradually found a place in industry since the late sixties and they provide an alternative to traditional processes such as distillation, extraction and evaporation. The application of these processes in the food industry can be considered as an emergent technology. Membrane technology has many advantages when compared to conventional separation techniques. One of them is that separation can be performed at room temperature and therefore it is adequate for heat-sensitive products, yielding a better quality product. Besides, operating, maintenance and manufacturing costs are lower than those of heat processes. Its use can be carried out in a continuous or discontinuous way and it allows combination with other processes [3].

The process of nanofiltration (NF) in non-aqueous applications is quite recent. It can replace traditional separation processes used in the chemical, pharmaceutical and biotechnological industries, where organic solvents are used in the production of certain products. Several studies on the application of NF commercial membrane in non-aqueous media have been reported [4,5]. In their review, Wang et al. [6] provides an overview of the some advance of solvent resistant Nanofiltration membrane (SRNF) in the non-aqueous systems, including the preparation of SRNF. The development trend of SRNF and existing problems were discussed. Silva et al. [7] pointed out the fundamental challenge for organic solvent nanofiltration membranes is to achieve a membrane having high both, solvent compatibility and lifetime. The main problem in NF is the membrane stability when organic solvents are used as non-aqueous media (ethanol, acetone, hexane, etc.). The use of different commercial RO/NF membranes for separating cotton oil from hexane, ethanol, and isopropanol solvents was reported by Koseoglu et al. [8]. Only one of these membranes permeated hexane without being destroyed (polyamide material). Wu and Lee [9] investigated hexane removal from a crude soybean oil/hexane mixture by using porous UF

* Corresponding author. Tel./fax: 54 652446211.
E-mail addresses: lfirman@ing.unrc.edu.ar (L.R. Firman), aochoa@unsl.edu.ar (N.A. Ochoa), marchese@unsl.edu.ar (J. Marchese), cpagliero@ing.unrc.edu.ar (C.L. Pagliero).

0376-7388/$ - see front matter © 2013 Elsevier B.V. All rights reserved.
http://dx.doi.org/10.1016/j.memsci.2012.12.040

ceramic membranes obtaining nearly 20% oil retention. Solvent recovery from soybean oil/hexane miscellas at bench-scale using flat sheet polymeric commercially available membranes made from polysulfone and polysulfone/polyamide under different operational conditions was evaluated by Ribeiro et al. [10]. They found higher temperatures showed positive effects on the permeate flux, retention of oil and free fatty acids permeation. A process combining solvent extraction with membrane technology to recover the oil was studied by Kwiatkowski et al. [11]. Some studies about synthesis and characterisation of organic solvent-resistant NF membranes have been published. Stafie et al. [12] studied the permeation of sunflower oil/hexane mixtures in polyacrylonitrile–polydimethylsiloxane (PAN/PDMS) membranes. Good performance was obtained at $\Delta p = 7$ bar and $T = 22\ ^{\circ}C$. Considering miscella with 8 and 30% oil, the permeate fluxes were 12.5 and 2.5 l $m^{-2}\,h^{-1}$, respectively, with oil rejection between 80–96%. Darvishmanesh et al. [13] investigated the performance of four polymeric commercial NF membranes for the recovery of solvents from oil–solvent mixtures. The membranes were tested for permeation of several organic solvents and oil. Experimental results showed that these nanofiltration membranes have a high solvent resistant and a suitable oil/solvent separation performance. The flux behaviour of a dense commercial polydimethylsiloxane membrane with various vegetable oils under undiluted and hexane diluted conditions was studied by Manjula et al. [14]. They found hexane dilution improved the permeate oil flux in all the vegetable oils. However the dense PDMS membrane did not show any oil/hexane selectivity over the experimental range studied. Weibin et al. [15] prepared PDMS/PVDF and Zeolite PDMS/PVDF composite membrane to be used in hexane recovery from soybean oil/hexane miscella. Zeolite PDMS/PVDF membrane showed the best separation performance (at 1.7 MPa) a flux of 2.52 Kg $m^{-2}\,h^{-1}$ with 96% oil retention.

In the oil industry the deacidification process is important, not only for consumer acceptance of final product quality, but also for its economic impact in the production process. The FFA delivers undesirable qualities to crude oil: unpleasant taste and smell. Besides, they can cause corrosion and contamination when the oils are industrially used and also interfere with later glyceride processing if chemical conversions (biodiesel production or transesterification) are carried out. Conventional deacidification practice is to use either a physical or chemical process. Also, an enzymatic process can be carried out. Each of these processes has disadvantages, among them greater energetic demand, effluent generation and neutral oil loss. Membrane technology can be an alternative to these processes if membranes with the adequate characteristics for the simultaneous separation of oil–FFA in hexane are prepared. There are only a few works related to oil deacidification and disagreeable flavours removed by membrane technology. Raman et al. [16] described a process for solvent recovery and partial solvent deacidification from miscella using different commercial membranes. Bhosle et al. [17] used polymeric hydrophobic nonporous and hydrophilic nanofiltration (NF) membranes for the deacidification of model vegetable oils with and without addition of organic solvents. They found that the differences in molecular size, solubility, diffusivity and polarity between triacylglycerols and oleic acid appears to be insufficient for achieving direct deacidification in terms of reasonable selectivity and throughput with these two membranes. In order to remove some compounds that are responsible for oil's unpleasant flavour, without altering the virgin olive oil, different commercial membranes were applied by Bottino et al. [18]. They concluded that the UF Carbosep M1 membrane was the most suitable for softening the oil organoleptic features.

An ideal membrane for solvent recovery should combine specific properties, such as high oil retention and an adequate permeate flux, as well as mechanical, thermal and chemical resistances. Besides, it should have low free fatty acid (FFA) retention. The objective of the research described in this paper is to evaluate the tailor made membranes for their ability to remove hexane and separate oil and FFA. The results are compared with a commercial NF membrane. The influence of operational variables (transmembrane pressure, temperature and concentration) on membrane solvent/oil permselectivity as well as FFA removal is analysed.

2. Experimental

2.1. Materials

Degummed soybean oil was obtained from a local industry (OLCA SAIC, Córdoba, Argentina) and was used to prepare synthetic miscella solutions. The oil concentration in the oil/hexane miscella samples was varied from 10 to 35% w/w. Oil composition according to the supplier is detailed in Table 1. This oil composition was similar to those reported by Sipos et al. [19]. The average molecular weight of triglycerides was calculated using major fatty acids composition (12% palmitic acid, MW 256.4; 3.3% stearic acid, MW 284.48; 17.7% oleic acid, MW 282; 56% linoleic acid, MW 280.45; 10% linolenic acid, MW 278.43), resulting in an average molecular weight of triglycerides, MW = 862.7 g mol^{-1}.

Non-woven Viledon 2431 support was provided by Carl Freudenberg (Weinheim, Germany). Poly(vinylideneflouride) (PVDF) high viscosity Solef 1015 supplied by Solvay (Brussels, Belgium) and dimethylformamide (DMF) purchased from Aldrich (Buenos Aires, Argentina) were used for preparing an asymmetric membrane. Analytical reagent-grade chloroform, ethanol, isopropanol, and n-hexane were used as supplied.

The coating materials were commercial poly-dimethylsiloxane (Siloc, Anaeróbicos S.A., Buenos Aires, Argentina) and cellulose acetate M_r 61,000 (Aldrich, Argentina). Siloc specifications before curing are: tixotropic dense (density 1.02 g cm^{-3}) and transparent paste, and after curing: aspect as gum very flexible and adhesive, tensile strength 1 to 1.5 MPa; elongation at break 250 to 400%; hardness 25 Shore-A; thermal conductivity 0.4–0.5×10^{-3} cal $cm^{-1}\ ^{\circ}C^{-1}\ s^{-1}$. As this is a commercial

The dyes used in the membrane molecular weight cut-off experiments were Methylene Blue (MB) (MW 374 g/gmol, 99%) and Rose Bengal (RB) (MW 1017 g/gmol, 99%). MB was purchased

Table 1
Degummed soybean oil composition and oil–FFA solubility parameters.

Compounds	Wt (%)	$\sum E_c$ (J/mol)	$\sum V$ (cm^3/mol)	δ_i ($MPa^{1/2}$)
Triglycerides	98.5			18.9
Trioleina		293,792	781.2	
Trinoleina		290,012	651.6	
Trioestarina		297,572	910.8	
FFA	0.5			17.9
Oleic acid	0.12	110,120	314.4	
Linolenic acid	0.035	107,600	304.0	
Linoleic acid	0.265	108,860	309.2	
Palmitoleic acid	1.56e-3	100,240	282.2	
Lauric acid	5.20e-4	81,740	223.0	
Miristic acid	1.05e-3	91,620	255.2	
Palmitic acid	0.056	101,500	287.4	
Stearic acid	0.020	111,380	319.6	
Araquidic acid	1.05e-3	121,260	351.8	
Sterols	0.33	135,310	301.2	
Tocopherols	0.18	152,831	285.0	
Squalene	0.014	138,800	363.0	

from Anedra S.A. (Argentina) and RB from Cicarelli Laboratories (Argentina).

2.2. Membranes

2.2.1. Asymmetric membrane preparation

The flat asymmetric membrane was prepared by the phase inversion process. Polymer solution, 23% w/w PVDF in dimethylformamide (DMF), was cast onto a non-woven Viledon polymeric flat support, at 25 °C in air (45–50% relative humidity), by using a film extensor with a 400 μm knife gap. After 20 s of solvent evaporation, the nascent membrane was immersed in a bi-distilled water coagulation bath (T=25 °C) for 1 h and then stored in fresh water. The asymmetric PVDF membrane was dried at room temperature for 48 h before being used.

2.2.2. Composite nanofiltration membrane preparation

To analyze the effect of hydrophobic/hydrophilic surface character on the composite membrane performance, two different coating materials were use in the tailor-made composite membranes; a hydrophobic PDMS polymer (Siloc) and a hydrophilic cellulose acetate (CA) polymer.

The Siloc material is a silicone sealant/adhesive of one component chemically reactive where the acetic cure is produced by the temperature, humidity, or heat. After acetic cure this material is transformed in a flexible and adhesive elastomer. As it is commercial product the exact chemical composition (dimethylsiloxane, hydroxy-terminated; fillers and plasticizers) was not provided by the supplier. The PVDF–PDMS composite membranes were prepared by covering the surface of the dried asymmetric PVDF membrane with a poly-dimethylsiloxane solution (film extensor gap of 200 μm, T=25 °C). The coating solutions were prepared by dissolving 10, 12 and 15 wt% of Siloc paste in hexane. The cross-linking reaction (acetic cure) of the poly-dimethylsiloxane coating was accomplished in an oven at 60 °C for 4 h. The composite membranes were identified as PVDF-10SI, PVDF-12SI and PVDF-15SI, respectively. The composite PVDF–cellulose acetate membrane (PVDF–CA) was prepared by covering the asymmetric PVDF support surface with a 0.2% w/w cellulose acetate in a chloroform solution (film extensor gap of 200 μm, T=25 °C). The chloroform solvent was eliminated by evaporating under ambient conditions. Higher CA concentration (i.e. 0.4 wt%) produced a hexane-tight composite membrane.

2.2.3. Commercial composite membrane

The commercial membrane selected for this study was Solsep 030306 silicone base polymer SOLESP® (Solsep-Apeldoom-The Netherlands), a composite nanofiltration flat membrane. This commercial membrane is reported by the provider as a solvent-resistant membrane for solvent recovery and it was previously tested to recover the solvent from soybean oil/solvent [13]. The membrane's molecular weight cut-off (MWCO) is 1000 Da in acetone/polystyrene according to the supplier. There is not much information available on the type of support material used for Solsep membrane preparation.

2.2.4. PVDF, PDMS and CA dense membranes

In order to corroborate the hydrophilic/hydrophobic characteristics of the polymeric materials, three dense membranes were synthesized from 5% w/w solutions of CA in chloroform, PDMS in hexane, and PVDF in DMF. The polymer solutions were cast onto a flat glass and the dense membranes were obtained after solvent evaporation under ambient conditions (T=298 K).

2.3. Liquid–liquid displacement porosimetry

Pore size distribution and molecular weight cut-off (MWCO) of PVDF support was determined by using the liquid–liquid displacement porosimetry technique (LLDP). Three liquids (mixture of isobutanol/methanol/water; 15/7/25, v/v/v) (surface tension, γ=0.35 mN/m) are used to pores analysis by applying relatively low pressures [20]. Procedure consists on filling the membrane with a liquid (wetting liquid, aqueous phase) and then displacing it from pores with the organic phase (isobutanol saturated with water and methanol). Flux through the membrane is obtained by using a syringe pump (ISCO 500D) to gradually increment the flux on the organic-phase side. Simultaneously, equilibrium pressure is measured in each incremental stage using a pressure transducer (OMEGA DP200). When the applied pressure and flux through the membrane were monitored, then the radii of opened pores at each applied pressure can be calculated from Cantor's equation. This equation is valid if we assume the liquid effectively wets the membrane (i.e. with null contact angle).

$$r_p = \frac{2\gamma}{\Delta p} \tag{1}$$

where Δp=applied pressure, γ=interfacial tension and r_p=pore equivalent radium. Assuming cylindrical pores, Hagen-Poiseuille relationship can be used to correlate volumetric flow (Q_i) of the pushing liquid and the number of pores, nk (k=1,…,i) having pore radii, rk ($<ri$). For each pressure step, Δpi, the corresponding measured volume flow is correlated with the number of pores thus opened by [20]:

$$Q_i = p_i\left(\frac{\pi}{8\eta l}\sum_{k=1}^{i} n_k r_k^4\right) \tag{2}$$

where ℓ is the pore length which corresponds to the active layer thickness and η the displacing fluid viscosity.

2.4. Contact angle measurements

The hydrophobic character of the membranes was determined by measuring the water–membrane contact angle (θ) by the sessile-drop technique using a contact angle device (Micromeritics Instrument Corporation, Norcross, GA, USA). Three drops of water were measured for each membrane sample. The contact angle value was measured 3 min after dropping water on the membrane surface. The average contact angles (θ) were evaluated from the following expression (User manual of Micromeritics' contact angle device)

$$\cos\theta = 1 - \sqrt{\frac{Bh^2}{\left(\left(1 - Bh^2/2\right)\right)}} \tag{3}$$

where $B=\rho g/2\gamma$, being "g" the gravity acceleration (980 cm/s^2), "ρ" bide stilled water density (0.9971 g/cm^3), "γ" interfacial tension of bi-distilled water (71.97 erg/cm^2), and h the height of the liquid drop.

2.5. Dye rejection tests

The MWCO of the PVDF–SI and PVDF–CA composite membranes were estimated in the dead end setup described in Section 2.6. The membranes were pre-conditioned with pure solvents of decreasing polarities following the procedure given in Section 2.7. Experiments were performed by triplicate at 10 bar of transmembrane pressure and T=303 K using 7.5×10^{-5} M Methylene Blue and 5.5×10^{-5} M Rose Bengal feed solutions in ethanol. Dye concentrations were determined by absorption spectrometry using UV–visible

spectrophotometer (Metrolab 330) at 664 nm and 548 nm for Methylene Blue and Rose Bengal, respectively.

The dye rejection values (%R) were evaluated from

$$\%R = \left(1 - \frac{C_p}{C_R}\right) \times 100 \quad (4)$$

where C_p and C_R are the dye concentration in the permeate and retentate respectively until the steady state flux was reached ($\approx$40 min).

2.6. SEM–EDS measurements

The composite membrane surface and cross section morphologies were observed using a scanning electron microscope (SEM) LEO 1450VP, and for EDS Genesis 2000 (EDAX) energy dispersion X-ray analysis. For the SEM morphological surface and cross section analysis, samples were coated by sputtering a thin gold layer. They were observed under high vacuum and EDS surface measurements were obtained applying an acceleration voltage of 120 kV.

2.7. Permeation of pure solvent and oil/hexane mixtures

The permeation experiments were performed in a dead-end filtration set-up described elsewhere [21]. The stainless steel 316L test cell (Sterlitech HP 4750, USA) has an inner diameter of 5.1 cm and height of 19.9 cm. The membrane was supported on a sintered porous stainless-steel disc. Membrane diameter was 4.9 cm with an effective area $A = 14.6 \times 10^{-4}$ m^2. To minimise the fouling phenomena the oil/hexane feed solution was stirred with a magnetic bar (500 rpm) placed over the membrane surface. Transmembrane pressure (Δp) was supplied by a nitrogen cylinder connected to the top of the cell. The experimental temperature was kept constant by the temperature-controller of the magnetic stirrer.

All membranes were pre-treated before the permeation experiments to minimise the effect of hexane on their structure. After the membranes were placed in the stainless steel module, they were flooded during 24 h with pure solvents of decreasing polarities; ethanol, isopropanol and hexane [22]. To gain a better idea of the stability and durability of the membranes in hexane, the structure of small membrane samples (2 cm $\times$ 2 cm) was observed visually after exposure to hexane during 48 h. No significant structural changes, such as crack-like openings on its surface and the swelling or shrinking of its structural matrix were observed for any of the membranes.

2.7.1. Pure solvent permeation

The hexane flux through the pre-treated membranes was determined in the dead-end filtration set-up described above. Each experiment was carried out in triplicate. The unit was operated in batch mode by charging the reservoir cell with pure organic solvent, and solvent flux through the membrane was measured as a function of transmembrane pressure (Δp=5–20 bar) at different temperatures (T=30, 40 and 50 °C). Permeate flux J (L/h^{-1} m^{-2}) was determined by measuring the permeate solvent volume accumulated (ΔV) during the operation time (Δt) at the steady-state conditions and calculated from:

$$J = \frac{1}{A}\frac{\Delta V}{\Delta t} \quad (5)$$

2.7.2. Soybean oil/hexane miscella permeation

The cell reservoir was charged with 270 cm^3 of oil/solvent mixture and stirred at a constant speed of 500 rpm. The variable parameters analysed in the oil-hexane separation performance experiments were transmembrane pressure (10, 15 and 20 bar), operating temperature (T=30, 40 and 50 °C), and oil feed miscella concentration (C_f=10–35% w/w). All permeation trials were carried out in triplicate and mean values of permeate flux (J) determined by Eq. (5) were reported. Membranes were reused after each permeation experiment. In order to reach the initial membrane solvent flux, membranes were cleaned in situ according to the following protocol: the membrane was rinse stirred for 1 h with pure isopropanol, and then the isopropanol was replaced by pure hexane and stirred for 1 h. Finally, the cell was filled with hexane and allowed to permeate for 40 min at a pressure of 20 bars and a temperature of 30 °C.

Oil concentration was determined with an UV absorption spectrophotometer (Metrolab 330) at a wavelength of 458 nm [9]. Free fatty acid (FFA) concentration was determined according with the AOCS Ca 5a-40 method using an automatic titrator (848 Titrino plus-Metrohm AG). The oil separation performance was evaluated from the oil retention factor %R (Eq. 4) with the oil concentrations in permeate (C_p) and retentate (C_r).

3. Results and discussion

3.1. PVDF support and composite membranes characteristics

Fig. 1(a) shows the pore size distribution obtained from the LLDP permeability data of PVDF support with a mean pore

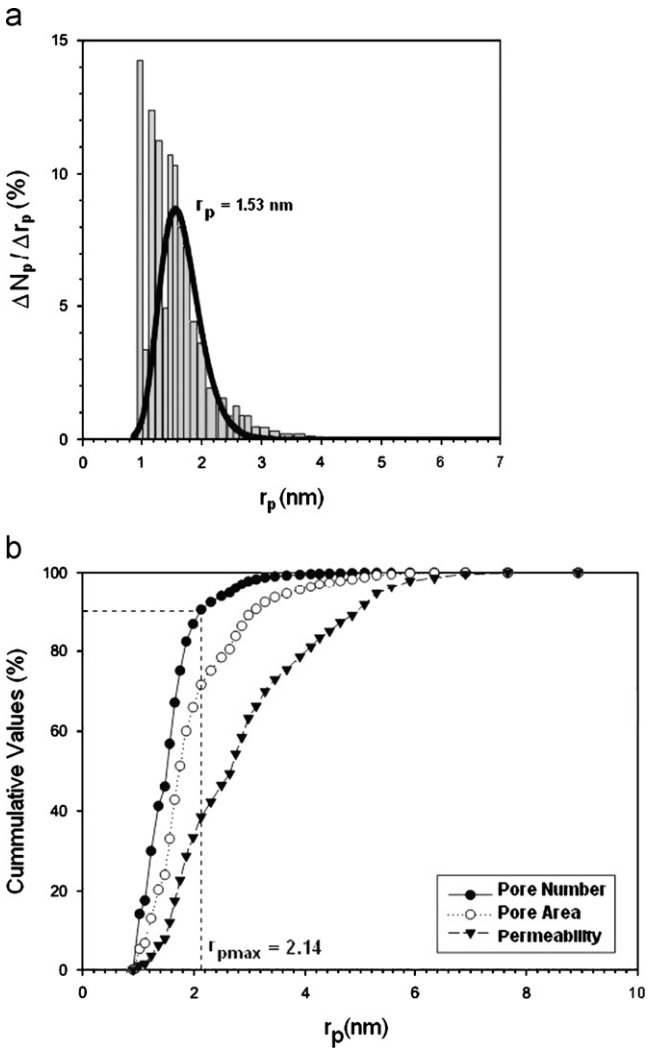

Fig. 1. Pore radius distribution (a) and molecular weight cut-off estimation (b) of PVDF support from LLDP.

diameter in the range of NF process ($r_p \approx 1.5$ nm). This distribution has been achieved by accounting for the contribution of each experimental step of flow-pressure increment to the overall membrane permeability (Eq. 2). Fig. 1(b) shows cumulative distributions for permeability, pore numbers and pore area. In order to estimate the MWCO, the pore size corresponding to the 90% biggest pores ($r_{p,max}$=2.14 nm) was determined from interception of the cumulative number of pores distribution (at 90%) with the r_p value in the ordinates axis [20]. To convert pore size ($r_{p,max}$) value into the equivalent molecular weight (MW) for a dextran molecule the following expression was used.

$$r_p = 0.33\ \mathrm{MW}^{0.46} \quad (6)$$

where MW is taken in Dalton (g/mol) and the pore size is given in Angstrom (Å). The MW≡MWCO=8.46 KDa obtained for $r_{p,max}$ is included in Table 2.

Table 2 also shows the membrane contact angles and the colourant rejection factors with their standard deviation. The values of contact angle for pure polymers denote the semi hydrophilic character ($50 < \theta < 70$) of dense CA and PVDF, and composite PVDF–CA related to the contributions of hydroxyl and flour groups; and the hydrophobic character ($\theta > 70$) of PVDF–SI composites and dense PDMS associated to van der Waals interactions. From the contact angles values of composite PVDF–SI membranes, it can be seen that there is a consistent increase in the hydrophobic characteristic with the increasing percentage of PDMS (θ from 103 to 118).

High rejection factors for Rose Bengal ($R > 90\%$) with the PVDF–12SI and PVDF–15SI composite membranes were achieved. Despite of the several membrane–dye factors that could affect the dye rejections (swelling, solubility, affinity, etc.), it could be assume that the molecular weight cut-off of these nanofiltration membranes are near to MWCO ≈ 1000 Da. The RB rejection values obtained for PVDF–10SI ($R \approx 68\%$) and PVDF–CA ($R \approx 63\%$) indicate that both membranes have MWCO higher than 1 KDa.

3.2. SEM micrographs and EDS results

Fig. 2 a–c illustrates the surface microphotographs of PVDF–10SI–12SI–15SI composite membranes, where two well defined bright and dark zones are present. The dark zone indicated that membrane support surface (PVDF) was not totally covered with a thick layer of the PDMS coating material. This fact would generate several coexisting flux resistances that contributed to the total effective flux resistance. Fig. 2 b shows a more homogeneous textural surface of PVDF–12SI composite membrane. From PVDF–SI surfaces it could infer that when the Siloxane concentration is 10% the amount of coating material is not sufficient to obtain a homogeneous coating layer; whereas a Siloxane concentration of 12% and 15% allow achieving a thicker and more uniform coating layer with high fissures and imperfections. These defects can be attributed to interfacial and contraction strengths of the siloxane material during the coating and curing process. Micrographs of cross section of PVDF–SI membranes (Fig. 2 d–f) shows there was not a clear boundary between the top layer and the PVDF support layer, indicating a tough adhesion between coating layer and support surface. The coating thickness increases (≈1, 2.5 and 3.5 μm) with the PDMS percentage (10, 12 and 15% SI).

Table 2
Contact angles, colourant rejections, and molecular weight cut-off.

Membrane	Θ	R%		MWCO (Da)
		MB	RB	
PVDF support	–	–	–	8460[b]
PVDF–10SI	102.8 ± 2.8	31.9 ± 2.5	67.96 ± 3.7	> 1000
PVDF–12SI	116.9 ± 3.5	74.8 ± 3.6	92.05 ± 4.6	~1000
PVDF–15SI	118.2 ± 4.1	88.8 ± 5.1	96.09 ± 5.3	~1000
PVDF–CA	58.1 ± 3.3	28.9 ± 4.3	62.50 ± 6.2	> 1000
Solsep 030306	95.0 ± 2.7[a]	–	–	1000[a]
PVDF(dense)	62.1 ± 1.5	–	–	–
PDMS (dense)	120.3 ± 3.6	–	–	–
CA (dense)	56.2 ± 1.2	–	–	–

[a] From Reference [7],
[b] From LLDP measurements.

SEM results were complete through the EDS measurements. Fig. 3 illustrates the SEM of PVDF–15SI membrane surface image and EDS spectra of dark and bright zones. Six samples of each composite membrane surface in $5 \times 5\ \mu m^2$ areas were analyzed. Table 3 shows the component average weight percentages and their standard deviations (SD) found in each composite membrane surface. Silicon (Si) and Fluorine (F) elements were identified on the whole surface to a greater or lesser extent, demonstrating that the PVDF surface was covered in different degree by the siloxane coating. In the dark-bright surface samples of PVDF–CA composite membrane and the commercial Solsep membrane, similar weight percentages of components were detected, indicative of both membrane surfaces were uniformly layered by the coating material.

3.3. N-hexane permeation

One of the parameters used to describe membrane integrity and design calculus is the permeability of pure hexane solvent. Solvent J values calculated from Eq. (7) were used to evaluate n-hexane permeability, L_h, from Darcy's law as follows:

$$J = L_h \Delta p = \frac{\Delta p}{\mu R_m} \quad (7)$$

where R_m is intrinsic membrane resistance, and μ is solvent viscosity.

Various hypotheses are available to describe the filtration mechanism for solvent-resistant NF membranes. Some authors mention the existence of solution-diffusion transport mechanisms [12,23], while others mention a convective pore flow mechanism [24,25]. Other researchers have proposed intermediate approximations between these two mechanisms [5,26]. Fig. 4 shows the average flux at different transmembrane pressures and the intrinsic support and membrane resistance values obtained from the slope of J versus $\Delta p/\mu$. Good concordance on the effect of pressure in the permeation of solvent according to Darcy's law can be observed, corroborating that the solvent transport through the membranes was mainly due to convective mechanism. The linearity of hexane flux with applied pressure also point out that no compaction of the membrane occurs over the applied pressure range. Comparing the support and composite membrane resistances (Fig.4), it can be observed that as the siloxane concentration increase from 0% to 15% the resistance to the passage of hexane increases. The increasing hexane flux resistances (PVDF–15SI > PVDF–12SI > PVDF–10SI > PVDF) could be attributed two main factors; (i) the surface pores of the PVDF support were covered with the PDMS coating material to different extents and, (ii) the higher coating layer thickness achieved with the increasing PDMS concentration (Fig. 2).

The average permeabilities of pure hexane (L_h) at different temperatures are included in Table 4. The L_h data were obtained from hexane flux at different Δp using Eq. (7) and the pure hexane viscosity (μ=0.3, 0.27 and 0.24 cP at 30, 40, and 50 °C, respectively). The permeability is strongly dependent on both the hydrophilicity of the membrane and the solvent used. The hydrophilicity/hydrophobicity of the membrane surface and the solvent polarity determine, to a great extent, the flux through

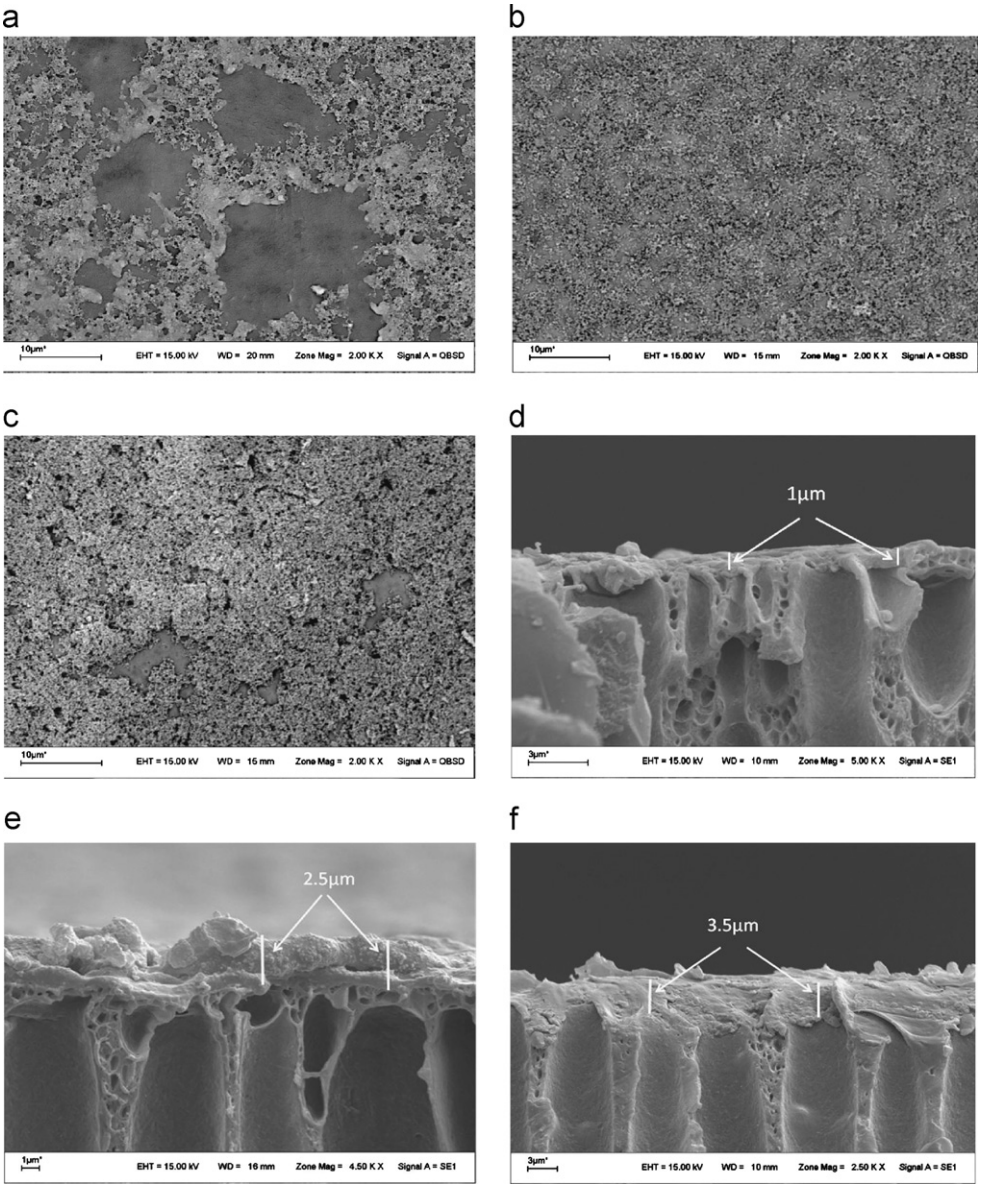

Fig. 2. Surface and cross section SEM images: (a), (d) PVDF–10SI; (b), (e) PVDF–12SI; and (c), (f) PVDF–15SI.

the membrane. The PDMS material ($\theta \approx 120$) is more hydrophobic than the CA material ($\theta \approx 56$). From contact angle measurements, the PVDF–SI membrane surfaces are more hydrophobic than the PVDF–CA composite membrane surface (Table 2), favouring permeation of low polar hexane solvent. This is not shown in Table 4 — PVDF–CA permeability to hexane was between 1.3 to 2.2 times higher than that of PVDF–SI. This higher permeability of hexane trough PVDF–CA could be explained as PVDF–CA has larger effective pore size than PVDF–SI as shown by the RB dye rejection experiments, $R\%$ (PVDF–CA) $< R\%$ (PVDF–SI) (Table 2). Table 4 also shows temperature effects on hexane permeability. Higher temperatures increased membrane hexane permeability, most likely because of the reduction of solvent viscosity with temperature.

3.4. Soybean oil/hexane miscella permeation

Fig. 5 shows the variation of permeate flux with time through the composite membranes at $T=30\,^{\circ}C$, $\Delta p=20$ bars and $C_f=25$ wt%. There was a moderate drop in permeate flux (around 10–15%) through the PVDF–SI membranes during the experimental time (90 min). For PVDF–CA and Solsep membranes the permeate flux decreased considerably during the first 20 min (30% and 65% respectively) and after that it practically remained constant. This behaviour implies that the membrane resistance changes during the initial NF process, possibly because of concentration polarisation phenomenon and development of an oil gel-layer on the membrane surface. After 40–60 min of operation time, similar flux decline behaviour was observed in every one of the experimental runs. This behaviour can be in part attributed to permeation operational mode. As it was mentioned in Section 2.7, the stirred dead-end cell was operated in batch mode operation, so the oil concentration in the permeation cell increases steadily with operation time, leading a gradually decrease of permeate flux. Permeate flux is an important factor in membrane processes since it directly affects its economy. The miscella permeate flux values at $t=60$ min, J^*, were used as reference fluxes to evaluate the effect of pressure, temperature, and oil concentration on membrane permselectivity properties. Table 4 summarises the J^* and oil rejection average values obtained with an oil/hexane feed concentration of 25% at different operational conditions for

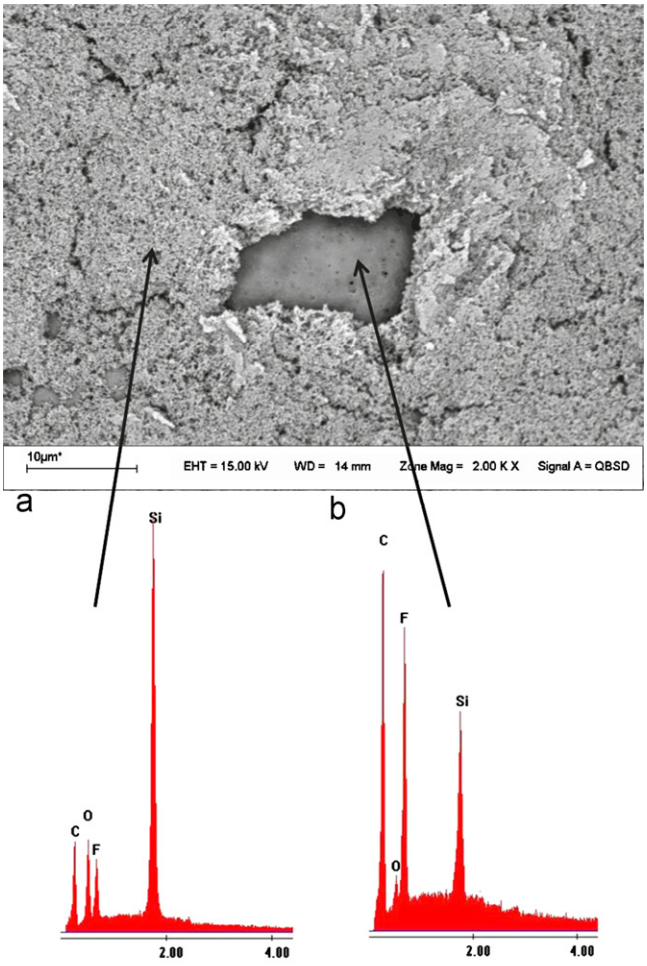

Fig. 3. SEM of PVDF–15SI membrane surface image and EDS spectra of two zones: (a) bright; and (b) dark.

Table 3
Weight element of membrane surfaces from EDS analysis.

Membrane	Element	Wt% (SD)	
		Bright zone	Dark zone
PVDF–10SI	C	50.5 (1.3)	58.0 (6.1)
	O	5.6 (2.0)	5.3 (3.9)
	F	25.1 (4.7)	29.4 (1.9)
	Si	18.8 (3.1)	7.3 (3.9)
PVDF–12SI	C	44.8 (7.2)	52.0 (4.1)
	O	12.2 (4.5)	7.9 (3.6)
	F	6.2 (2.4)	10.9 (3.7)
	Si	36.8 (5.2)	29.2 (4.6)
PVDF–15SI	C	32.4 (8.3)	64.6 (0.3)
	O	17.3 (4.0)	2.7 (1.1)
	F	5.2 (3.4)	23.0 (1.4)
	Si	45.1 (9.5)	9.7 (0.5)
PVDF–CA	C	57.9 (3.1)	57.4 (2.5)
	O	3.2 (1.2)	3.1 (0.8)
	F	38.9 (2.4)	39.5 (3.7)
Solsep 030306	C	68.3 (1.6)	66.8 (1.3)
	O	16.4 (2.1)	17.5 (1.9)
	Si	4.8 (0.8)	5.4 (1.0)
	Ti	10.5 (1.1)	10.3 (0.6)

the PVDF–SI, PVDF–CA, and Solsep composite membranes. Increasing the pressure from 10 bar to 20 bar increased permeate flux indicating the flux is controlled by pressure the effect of

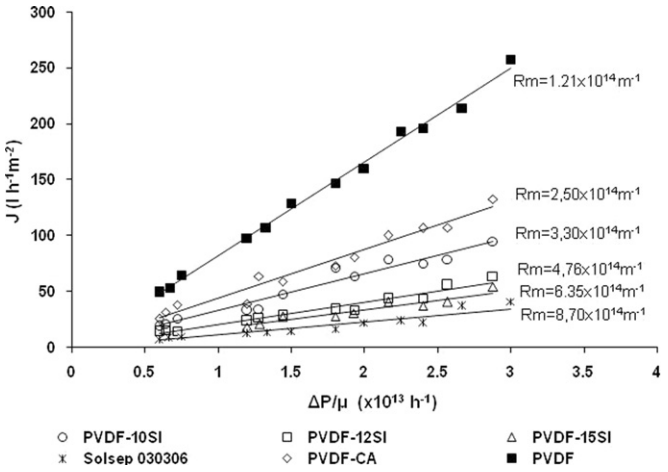

Fig. 4. Effect of transmembrane pressure (Δp) on hexane flux (J) of synthesized and commercial membranes.

concentration polarisation being low in the applied pressure range. Besides, it can be observed that permeate flux increases with an increase in temperature because a decrease in the viscosity of the feed miscella and an increase in the polymeric chains mobility, which brings about an increase in macromolecule diffusion.

There is a reasonable oil–hexane flux decrease with the increasing amount of coating siloxane material. The PVDF–15SI membrane showed lower oil–hexane flux and similar oil rejections than the PVDF–12SI. This could be explained considering two opposite effects, (i) the surface pores of both membranes were cover in similar extent by the siloxane material (similar membranes cut-off), and (ii) the higher thickness of PVDF-15SI coating layer compare to the PVDF–12SI one. This explanation is supported by the SEM micrographs (Fig. 2 e,f) and dye rejections data (Table 2).

Membrane performance relative to oil rejection was evaluated according with Eq. (2). Table 4 shows the variation of oil rejection values from 20 to 84.6 wt%. The PVDF–12SI membrane showed the highest efficiency for oil/hexane separation (at C_f=25%, Δp=20 bar, and T=30 °C) combining high permeate flux (J^*=20.3 l/m^{2}h) and high oil rejection (%R=80); therefore, these operational condition were chosen for further studies of feed oil concentration effect on FFA–oil membrane permselectivity. Table 5 illustrates membrane fluxes and the rejection data using different feed oil concentrations at a pressure of 20 bar and a temperature of 30 °C. From these values it is clear that the miscella permeability decrease when the feed oil concentration increases. A higher miscella concentration in the feed implies an augment in the quantity of dissolved solutes, increasing the fouling and concentration polarization effects, which in turn produce an increase in the total membrane resistance. This effect and the increasing viscosity of the miscella leads to a reduction in J^* permeate flux as oil concentration increases.

As it was mentioned in the introduction section, good oil rejection performance was obtained by Stafie et al. (PDMS/PAN membrane) [12] and Weibin et al. (Zeolita PDMS/PVDF membrane) [15]. In these cases, the performance of PVDF–20SI membrane related to oil retention was lower compared with those of Stafie et al. [12] (87–90%) and Weibin et al. [15] (96%), however the permeate fluxes of PVDF–12SI were 6.3–2.9 times and 5.6 times higher than PDMS/PAN and Zeolita PDMS/PVDF membranes, respectively. The relatively low flux recovery of PDMS/PAN and Zeolita PDMS/PVDF membranes compared with PVDF–12SI one could be in part attributed to the different

Table 4
Pure hexane permeability, miscella permeate flux and oil retention.

Membrane	T (°C)	Δp (bar)	Lh ± l/(hm²bar)	J* l/(hm²)	%R
PVDF–10SI	30	20	3.61 ± 0.34	20.1	76.8
		15		16.5	76.1
		10		12.5	68.0
	40	20	3.96 ± 0.32	22.9	74.0
		15		18.5	70.4
		10		14.0	67.7
	50	20	4.91 ± 0.37	24.4	71.6
		15		18.7	69.4
		10		14.4	62.8
PVDF–12SI	30	20	2.25 ± 0.22	20.3	80.0
		15		15.9	84.6
		10		10.9	80.6
	40	20	2.59 ± 0.26	20.9	72.7
		15		15.9	82.0
		10		13.5	70.0
	50	20	3.03 ± 0.29	19.7	80.8
		15		17.0	80.6
		10		12.7	79.5
PVDF–15SI	30	20	1.85 ± 0.29	15.6	80.3
		15		10.9	79.7
		10		7.8	81.3
	40	20	2.02 ± 0.23	16.1	78.7
		15		11.7	79.8
		10		8.1	80.5
	50	20	2.70 ± 0.30	19.1	77.3
		15		15.3	79.2
		10		10.5	80.1
PVDF–CA	30	20	4.76 ± 0.44	14.9	48.5
		15		14.2	44.3
		10		11.3	39.4
	40	20	5.53 ± 0.45	19.0	55.0
		15		16.9	38.0
		10		13.2	36.7
	50	20	6.79 ± 0.52	19.9	38.5
		15		18.4	41.3
		10		14.8	38.0
Solsep 030306	30	20	1.12 ± 0.09	4.9	54.1
		15		4.7	32.5
		10		4.7	24.8
	40	20	1.66 ± 0.16	6.8	35.7
		15		5.8	35.9
		10		5.2	25.5
	50	20	1.82 ± 0.15	7.6	33.9
		15		6.5	30.7
		10		5.6	19.7

J^* = permeate flux at t = 60 min; C_f = 25% w/w oil/hexane.

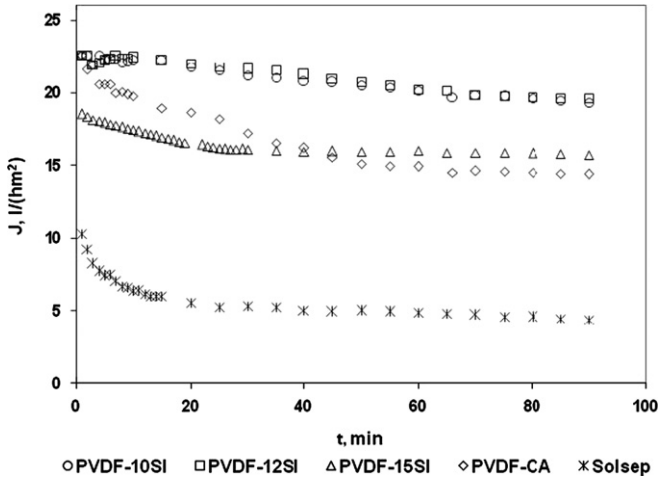

Fig. 5. Soybean oil/hexane flux time dependence at Δp = 20 bar, C_f(oil) = 25% w/w, and T = 30 °C of synthesized and commercial membranes.

thickness of the coating layer and operation conditions (temperature, pressure, feed oil concentration, oil characteristics, etc).

3.5. FFA membrane separation efficiency

In order to determine the PVDF–12SI membrane performance on FFA separation, the separation efficiency or sieving efficiency, (β_i), was used. This factor is defined [27,28] as:

$$\beta_i = 1 - R_i = \frac{C_{pi}}{C_{Ri}} \tag{8}$$

where C_{pi} and C_{Ri} are the oil or FFA concentration in the permeate and retentate respectively. If the efficiency factor of solute is higher than one, the component will preferably permeate through the membrane; if it is lower than one it would preferentially be retained by the membrane. The oil and FFA separation efficiency data as a function of pressure at different temperatures for the PVDF–12SI membrane are reported in Fig. 6. General trends indicated that the FFA separation efficiency increased as the trans-membrane pressure increased being practically constant

Table 5
Effect of oil feed concentration on permeate flux and oil rejection ($\Delta p=20$ bar, $T=30$ °C).

Membrane	C_f (wt%)	C_P (wt%)	C_R (wt%)	J^* l/(hm^2)	%R
PVDF–10SI	10	3.92	10.45	33.2 ± 2.5	62.5 ± 4.4
	25	6.86	29.58	20.1 ± 1.7	76.8 ± 3.0
	35	9.29	36.86	14.7 ± 1.9	74.8 ± 2.7
PVDF–12SI	10	2.27	11.57	30.3 ± 1.9	80.4 ± 3.5
	25	5.43	27.17	20.3 ± 1.2	80.0 ± 4.1
	35	6.39	37.07	15.2 ± 1.3	82.7 ± 2.5
PVDF–15SI	10	2.39	12.32	21.5 ± 1.7	80.6 ± 3.0
	25	5.61	28.50	15.6 ± 1.4	80.3 ± 2.7
	35	7.41	36.30	11.7 ± 1.1	79.7 ± 4.3
PVDF–CA	10	7.96	11.62	27.1 ± 2.3	31.5 ± 1.6
	25	14.37	27.90	14.9 ± 1.5	48.5 ± 2.4
	35	18.10	35.90	13.3 ± 1.3	49.3 ± 3.1
Solsep 030306	10	5.61	11.00	9.2 ± 0.8	49.9 ± 2.9
	25	12.47	27.10	4.9 ± 0.9	54.1 ± 2.3
	35	16.02	36.50	3.9 ± 0.5	56.1 ± 3.5

J^* = permeate flux at $t=60$ min; C_R,C_p = oil concentration in the permeate and retentate.

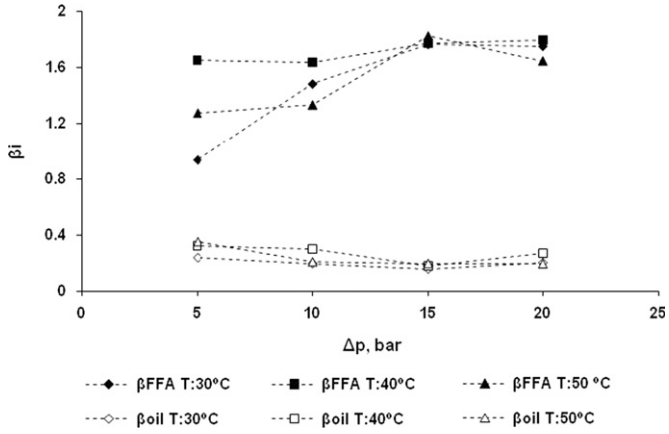

Fig. 6. Effect of transmembrane pressure (Δp) and temperature on FFA and oil separation efficiency for PVDF–12SI membrane.

at Δp higher than 15 bar. Although the oil separation efficiency values of the PVDF–12SI showed some variations, these were within the experimental error, so the β_{oil} can be considered constant for varying temperature and pressure. The best membrane separation performance was achieved at pressures of 15–20 bar, attaining β_{FFA} values up to 1.85 (high FFA permeation), and a β_{oil} value of 0.2 (high oil rejection). This behaviour can be attributed, among other factors, to: (i) FFA molecular weights (<300) lower than that of oil (>900) and, (ii) the different affinities FFA–hexane and oil–hexane have. To analyse the effect of solute–solvent affinity on oil and FFA separation efficiency, the solubility parameters (δi) [29,30] were determined by the group contribution method [31], according with $\delta i=(\sum E_c/\sum V)^{1/2}$, where E_c and V are the molar cohesive energy and molar volume, respectively. The $\sum E_c$, $\sum V$, and δi data for soybean oil compounds are given in Table 1. The hexane solubility parameter value, $\delta_{hexane}=14.9$ MPa$^{1/2}$, was evaluated from its cohesive energy ($\sum E_c=29{,}180$ J/mol) and molar volume ($\sum V=131.4$ cm^3/mol). The difference between $|\delta_{FFA}-\delta_{hexane}|=3$ was lower than $|\delta_{oil}-\delta_{hexane}|=4$, indicating that hexane was a better solvent for FFA solutes than oil components. In this case, the FFA tends to remain in the hexane phase, so, when the transmembrane pressure was increased the hexane flux increased, enhancing the FFA transport through the membrane and increasing its concentration in the permeate side. Lai et al. [29] have obtained the best FFA/oil separation with $\beta_{FFA}=2.12$ and $\beta_{oil}=0.24$ for soybean oil using a hybrid process; supercritical CO_2 process combined with nanofiltration process. In this study, a similar separation efficiency was achieved by the PVDF–12SI lab tailor-made composite membrane ($\beta_{FFA}=1.85$ and $\beta_{oil}=0.2$). In summary, an appropriate membrane design can lead to both an efficient hexane recovery and FFA–oil separation in just one process.

4. Conclusions

The results obtained in this study show that deacidification and solvent recovery from soybean oil/hexane miscella using nanofiltration composite membranes presents a high potential for application in the oil industry. Out of the five membranes under study, the PVDF–12SI membrane presented the best permselectivity characteristics, obtaining a permeate flux of 20.3 l/(hm^2) at $\Delta p=20$ bar, $T=30$ °C, and $t=60$ min. In these operating conditions, the soybean oil concentration decreased from 25 wt% in the feed to 5.4 wt% in the permeate reaching a soybean oil retention of 80% and a simultaneous reduction of 58% of the FFA in the original feed. Other key design parameter obtained from the PVDF–12SI was the separation or selectivity factor ($S(i/j)=\beta_i/\beta_j$). In this case, the FFA/oil and hexane/oil selectivity were $S_{FFA/oil}=\beta_{FFA}/\beta_{oil}=9.25$ and $S_{hex/oil}=\beta_{hex}/\beta_{oil}=6.6$.

From the comparative analysis between the membranes synthesised in our laboratories and the commercially available Solsep membrane, it can be observed that both a higher permeate flux and oil recovery were achieved when using PVDF–12SI membrane. The solvent-resistant physical tests showed that the PVDF–12SI membrane did not undergo significant changes in its structural and functional properties in the processing times.

The above results suggest that membrane technology can allows a high efficiency in the treatment of oil/hexane miscellas commonly processed in the oil industry.

Acknowledgements

The authors acknowledge the National Research Council of Argentina (CONICET) and National Agency for Scientific Promotion (ANPCyT) for their financial support.

References

[1] J.B. Snape, M. Nakajima, Processing of agricultural fats and oils using membrane technology, J. Food Eng. 30 (1996) 1–46.
[2] J.B. Woerfel, Extraction, in: D.R. Erikson (Ed.), Practical Handbook of Soybean Processing and Utilization, AOCS Press, Champaign, IL, 1995, pp. 85–89 United Soybean Board (St. Louis, MO).
[3] A.P.B. Ribeiro, N. Bei, L.A.G. Goncalves, J.C.C. Petrus, L.A. Viotto, The optimisation of soybean oil degumming on a pilot plant scale using a ceramic membrane, J. Food Eng. 87 (2008) 514–521.
[4] D. Bhanushali, S. Kloos, C.D. Kurth, D. Bhattacharyya, Performance of solvent-resistant membranes for non-aqueous system: solvent permeation result and modeling, J. Membr. Sci. 189 (2001) 1–21.
[5] D.R. Machado, D. Hasson, R. Semiat, Effect of solvent properties on permeate flow through nanofiltration membranes. Part I. Investigation of parameters affecting solvent flux, J. Membr. Sci. 163 (1999) 93–102.
[6] Wei Wang, XiangLi Fenjuan, Jin Wanqin, Xu Namping, Solvent resistant nanofiltration membranes, Prog. Chem. 19 (10) (2007) 1592–1597.
[7] P. Silva, L.G. Peeva, A.G. Livingston, Nanofiltration in Organic Solvents, in: N.N. Li, A.G. Fane, W.S. Winston, T. Matsuura (Eds.), Advanced Membrane Technology and Applications, John Wiley & Sons, New Jersey, 2008, pp. 451–465.
[8] S.S. Koseoglu, J.T. Lawhon, E.W. Lusas, Membrane processing of crude vegetable oils: pilot plant scale removal of solvent from oil miscellas, J. Am. Oil Chem. Soc. 67 (1990) 315–322.
[9] J.C. Wu, E. Lee, Ultrafiltration of soybean oil/hexane extract by porous ceramic membranes, J. Membr. Sci. 154 (1999) 251–259.

[10] A.P.B. Ribeiro, J.M.L.N. Moura, L.A.G. Gonçalves, J.C.C. Petrus, L.A. Viotto, Solvent recovery from soybean oil/hexane miscella by polymeric membranes, J. Membr. Sci. 282 (2006) 328–336.
[11] J.R. Kwiatkowski, M. Cheryan, Recovery of corn oil from ethanol extracts of ground corn using membrane technology, J. Am. Oil Chem. Soc. 82 (2005) 221–227.
[12] N. Stafie, D.F. Stamatialis, M. Wessling, Insight into the transport of hexane–solute Systems through tailor-made composite membranes, J. Membr. Sci. 228 (2004) 103–116.
[13] S. Darvishmanesh, T. Robberecht, P. Luis, J. Degrève, B. Van der Bruggen, Performance of nanofiltration membranes for solvent purification in the oil industry, J. Am. Oil Chem. Soc. 88 (2011) 1255–1261.
[14] S. Manjula, H. Nabetani, R. Subramanian, Flux behavior in a hydrophobic dense membrane with undiluted an.d hexane-diluted vegetable oils, J. Membr. Sci. 366 (2011) 43–47.
[15] Cai Weibin, Sun Yanzhi, Piao Xianglan, Li Jiding, Zhu Shenlin, Solvent recovery from soybean oil/hexane miscella by PDMS composite membrane, Chin. J. Chem. Eng. 19 (2011) 575–580.
[16] L.P. Raman, M. Cheryan, N. Rajagopalan, Solvent recovery and partial deacidification of vegetable oil by membrane technology, Lipid 98 (1996) 10–14.
[17] B.M. Bhosle, R. Subramanian, K. Ebert, Deacidification of model vegetable oils using polymeric membranes, Eur. J. Lipid Sci. Technol. 107 (2005) 746–753.
[18] A. Bottino, G. Capannelli, A. Mattei, P. Rovellini, P. Zunin, Effect of membrane filtration on the flavor of virgin olive oil, Eur. J. Lipid Sci. Technol. 110 (2008) 1109–1115.
[19] E.F. Sipos, B.F. Szuhaj, Aceite de Soja. Composición y propiedades físicas, in: Libro 10 ° Aniversario Aceites y Grasas Recopilación de artículos técnicos, ASAGA Ed., Argentina, 2000, pp. 52–58.
[20] J.I. Calvo, R.I. Peinador, P. Prádanos, L. Palacio, A. Bottino, G. Capannelli, A. Hernández, Liquid–liquid displacement porometry to estimate the molecular weight cut-off of ultrafiltration membranes, Desalination 268 (2011) 174–181.
[21] C. Pagliero, N. Ochoa, J. Marchese, M. Mattea, Degumming of crude soybean oil by ultrafiltration using polymeric membranes, J. Am. Oil Chem. Soc. 78 (2001) 793–796.
[22] N. Ochoa, C. Pagliero, J. Marchese, M. Mattea, Ultrafiltration of vegetable oils degumming by polymeric membranes, Sep. Purif. Technol. 22–23 (2001) 417–422.
[23] L.S. White, Transport properties of a polyimide solvent resistant nanofiltration membrane, J. Membr. Sci 205 (2002) 191–202.
[24] J.C. Whu, B.C. Baltzis, K.K. Sirkar, Nanofiltration studies of larger organic microsolutes in methanol solutions, J. Membr. Sci. 170 (2000) 159–172.
[25] J.P. Robinson, E.S. Tarleton, C.R. Millington, A. Nijmeijer, Solvent flux through dense polymeric nanofiltration membranes, J. Membr. Sci. 230 (2004) 29–37.
[26] M.F.J. Dijkstra, S. Bach, K. Ebert, A transport for organophilic nanofiltration, J. Membr. Sci. 286 (2006) 60–68.
[27] R.D. Noble, S.A. Stern (Eds.), Principles and Applications, Elsevier Science B.V., The Netherlands, 1995, pp. 54–55.
[28] S.J. Sarrade, G.M. Rios, M. Carles, Supercritical CO_2 extraction coupled with nanofiltration separation-applications to natural products, Sep. Purif. Technol. 14 (1998) 19–25.
[29] L.L. Lai, K.C. Soheili, W.E. Artz, Deacidification of soybean oil using membrane processing and subctritical carbon dioxide, J. Am. Oil Chem. Soc. 85 (2008) 189–196.
[30] S. Darvishmanesh, J. Degrève, B. Van der Bruggen, Mechanism of solute rejection in solvent resistant nanofiltration: the effect of solvent on solute rejection, Phys. Chem. Chem. Phys. 12 (2010) 13333–13342.
[31] D.W. Van Krevelen, K. te Nijenhuis, Properties of Polymers, Elsevier, The Netherlands, 2009, pp. 189–227.